Preparations for Tomographic Background-Oriented Schlieren at the 31-Inch Mach 10 Wind Tunnel

Brett F. Bathel*, Joshua M. Weisberger†, William H. Ripley‡
NASA Langley Research Center, Hampton, Virginia, 23681

Stephen B. Jones§
Analytical Mechanics Associates, Hampton, Virginia, 23681

This paper details efforts by researchers at NASA Langley Research Center to prepare for an upcoming high-speed tomographic background-oriented schlieren test entry in the 31-Inch Mach 10 wind tunnel. In order to troubleshoot potential problems that might arise when setting up the experiment in the actual test facility, a full-scale mock-up of the 31-Inch Mach 10 wind tunnel test section was constructed in the laboratory to provide equivalent characteristic optical access and mounting options. A 3D-printed model that replicates the scale of the forebody of a supersonic retropropulsion (SRP) model that will be used in the final test entry has been fabricated with a central nozzle that can be connected to a high-pressure gas supply to approximate the nozzle flow that will occur. Six high-speed imaging systems consisting of a high-speed camera with a fiber illuminator module have been assembled and mounted on the test section mock-up to provide six unique perspective views of the nozzle flow from the model. Tests with one of the imaging systems using a pulsed laser light source showed that sufficient signal intensity and illumination uniformity were achieved, as demonstrated by the 2D BOS data obtained with the system. Additional work to show that retroreflective material would survive inside of the test section of the 31-Inch Mach 10 tunnel was also performed. Finally, a remotely-controlled tomographic BOS calibration system is discussed.

I. Introduction

Background-oriented schlieren (BOS) is a semi-quantitative schlieren-based flow visualization technique [1], first introduced in the early 2000s [2–5], where a background pattern is first imaged without flow and then with flow. By measuring the apparent displacement in small regions within the larger patterned image with and without the flow, a two-dimensional displacement map can be computed. Typically, cross-correlation, iterative least squares (ILS), or optical flow algorithms are used to ascertain the displacements. Examples of correlation-based displacement maps can be found in Ref. [1], ILS in Ref. [6], and optical flow displacement maps in Refs. [6, 7]. These displacement maps are related to the path-integrated density gradient field that exists in the direction normal to the camera's optical axis and is present between the patterned background and camera lens. While BOS is considered to be semi-quantitative in nature (a path-integrated displacement map is obtained), tomographic BOS measurements have the ability to provide quantitative measurements of the density field (density value at each voxel element in a volumetric density field reconstruction). Examples of tomographic BOS measurements of the density or refractive index field can be found in Refs. [8–33]. Recent work with machine learning in the form of physics-informed neural networks (PINN) [34, 35] has extended the capabilities of the tomographic BOS method to include an ability to estimate the volumetric velocity and pressure fields in addition to the density field.

Planning for a tomographic BOS test in the 31-Inch Mach 10 wind tunnel (31M10) at NASA Langley Research Center is currently underway with an anticipated test date of fall, 2022. The primary goals of the test are to demonstrate the ability to acquire high-speed (≥50 kHz) multi-camera, two-dimensional, time-resolved BOS measurements in a high-speed ground test facility, and then use the BOS data from these cameras to generate a quantitative volumetric reconstruction of the density field in the test section. Since the freestream density in the 31M10 facility is relatively low

*Research Engineer, Advanced Measurements and Data Systems Branch, MS 63, AIAA Senior Member.
†Research Engineer, Advanced Measurements and Data Systems Branch, MS 63, AIAA Member.
‡Engineering Technician, Advanced Measurements and Data Systems Branch, MS 63.
§Electronics Technician, Advanced Measurements and Data Systems Branch, MS 63.

(4.4×10^{-3} – 1.6×10^{-1} kg/m^3), a model capable of producing a flow field with strong density gradients that does not obstruct any of the camera views is required. Previous conventional schlieren testing in the facility with a supersonic retropropulsion (SRP) model with a single, center nozzle [36] showed that the counter-flowing jet produced by the model produced relatively strong density gradient features over a large field-of-view without obstruction. It also demonstrated the need for high-speed imaging to adequately capture fast flow transients. Figure 1a shows an image of the SRP model with the center nozzle in NASA Langley Research Center's Unitary Plan Wind Tunnel Test Section 2 taken from Ref. [37]. Figure 1b shows a single image from the high-speed schlieren image sequence acquired of the counter-flowing jet issuing from the center nozzle on the SRP model in the 31M10. More details on this 70° sphere-cone model can be found in Ref. [37]. Since the counter-flowing jet of the model generates relatively strong density gradient structures over a large range of length scales, and since its 70° sphere-cone forebody allows for views of the flow from numerous unobstructed angles, it was selected as the model for use in this tomographic BOS demonstration test.

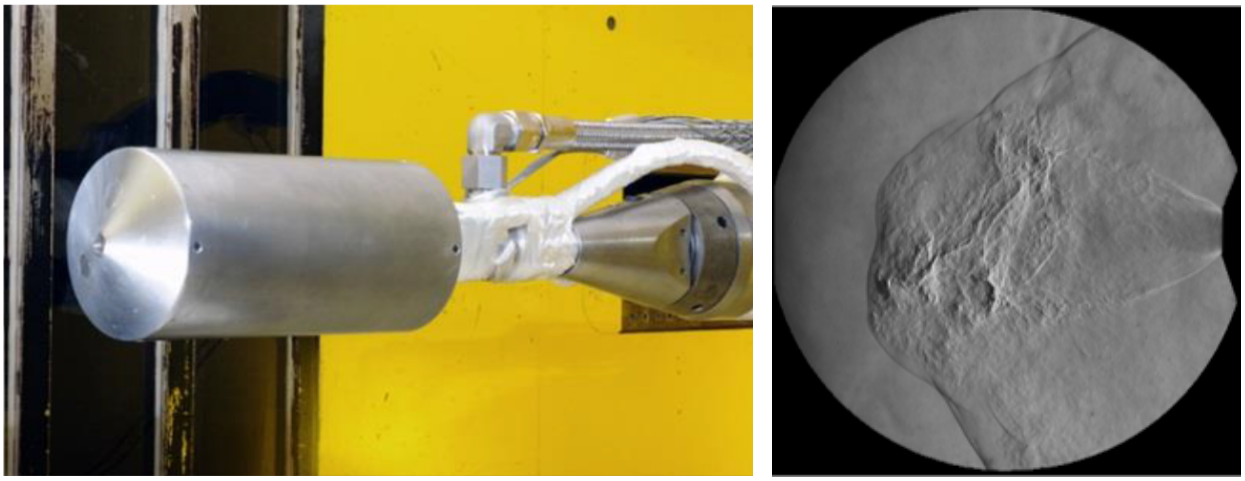

(a) **(b)**

Fig. 1 (a) Image of the SRP model with center nozzle configuration in the NASA Langley Research Center Unitary Plan Wind Tunnel taken from [37] and (b) single image from high-speed schlieren image sequence of counter-flowing jet issuing from SRP model in the 31M10.

Prior to conducting the tomographic BOS demonstration test in the 31M10, a significant amount of laboratory preparation work is required to ensure the test campaign is successful. Preliminary tests performed in 2019 [26] showed that it was possible to acquire relatively high-quality, time-resolved density field reconstructions when accounting for some of the optical access limitations that the 31M10 presents. In that work, four high-speed Photron™ SA-Z cameras were used to acquire BOS images of a helium jet, as shown in Fig. 2a. These cameras were arranged such that they mimicked the optical access that was expected when imaging through the top and side windows of the 31M10. Each camera was also equipped with a frame splitter – consisting of a 90° wedge mirror and two silvered mirrors – so that two unique perspective views of the helium jet, placed at a location corresponding to the tunnel's centerline, could be acquired with a single camera at half of the camera's resolution. Panels covered with retroreflective sheeting that were painted with a randomized pattern of black dots were placed such that they would correspond to the position of the tunnel walls opposite the top and side windows of the tunnel. Illumination was provided from a pulsed LED on each camera with the light being loosely collimated and diffused by a 2-inch-diameter condenser/diffuser lens. Figure 2b shows a time-resolved density field reconstruction obtained with this setup. While this preliminary work showed that tomographic BOS measurements might be possible when performed in the 31M10, it was determined that additional lab testing with a test section mock-up was needed in order to better capture the geometry and challenges of the facility.

The purpose of this paper is to provide details on laboratory work that has been performed in preparation for the planned high-speed tomographic BOS test in the 31M10. The following sections provide a description of aspects of the test and various components of the tomographic BOS measurement system that were considered during preparation for measurements in the facility. Improvements made to the setup relative to the preliminary work completed in 2019 are discussed as well. Finally, discussions of work to be completed prior to the final test entry are provided.

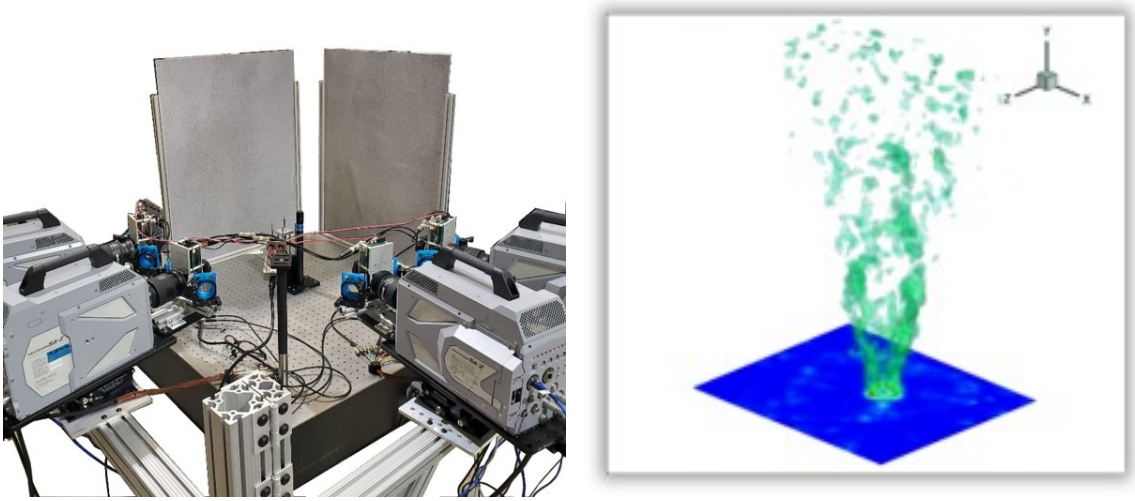

(a) (b)

Fig. 2 Preliminary (a) setup of high-speed tomographic BOS test in 2019 and (b) resulting time-resolved density reconstruction obtained with a helium jet.

II. Experimental Setup

A. 31-Inch Mach 10 Wind Tunnel Facility Mock-Up

The 31M10 at NASA Langley Research Center is a blow down air tunnel with a 31-inch × 31-inch square test section. Details on the facility can be found in Refs. [38, 39]. Optical access is provided on the top, side and bottom of the tunnel by Corning 7940 schlieren-quality fused silica windows. Model injection occurs through the remaining side wall once the freestream conditions in the tunnel have been established. Figure 3a shows (from top to bottom) the size and relative locations of the top, side, and bottom windows in the facility, as well as the injection plate that makes up the fourth wall of the test section.

In order to optimize camera placement to achieve the highest quality tomographic BOS measurements, a full scale mock-up of the 31M10 test section was constructed in the laboratory using 80/20™ t-slotted aluminum profiles and fasteners for the framing and Alumalite® panels for the tunnel walls. Cutouts were made in the Alumalite® panels to match the exact size and relative location of the top, side, and bottom windows in the facility, shown in Fig. 3b. The location of the injection plate was drawn onto the remaining panel to aid with model placement. A mounting platform was constructed next to the side window of the mock-up to mimic the platform that will be constructed next to the 31M10 facility for camera mounting. Additional 80/20® mounting hardware has also been included around the top and bottom windows to mimic the hardware that currently exists at 31M10. An adjustable sting assembly was also constructed out of 80/20™ t-slotted profiles for the mock-up that allowed for the model to be easily repositioned in the spanwise and streamwise directions using linear bearings that could be locked into place with handbrakes.

Figure 4 shows the laboratory mock-up of the 31M10 test section with six high-speed Photron™ SA-Z cameras mounted around the test section. In this image, the cameras have been positioned more uniformly around the test section compared to the arrangement shown in Fig. 2a, with three cameras mounted above the top window, two cameras mounted at the side window, and a sixth camera mounted below the test section. In this setup, each camera was secured to a 6-inch by 18-inch square breadboard (Newport™, SA2-06X18) that attached to an angled 30°/60° mounting bracket (Thorlabs™, AP30) using a modular base plate (Newport™, CB-2). This assembly was then mounted onto a pitch/roll/yaw stage (Huber™, Type 300 Model D) that was secured to the 80/20™ structure of the 31M10 mock-up. This allowed the camera orientation to be easily adjusted.

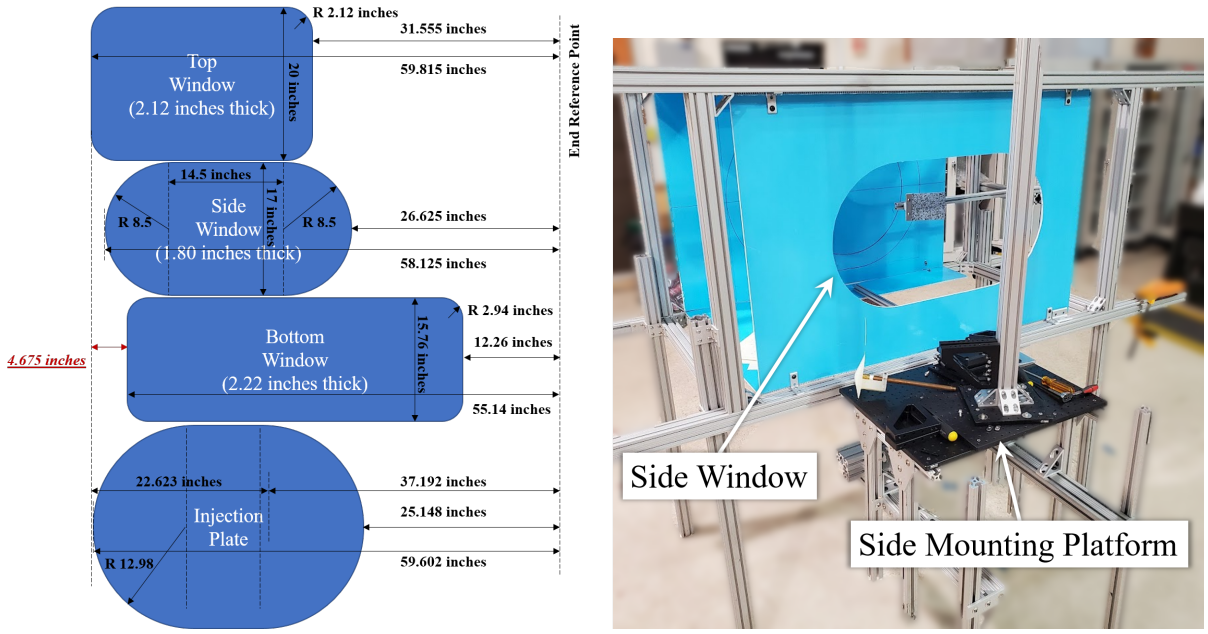

(a) **(b)**

Fig. 3 (a) Size and relative streamwise positions of top window, side window, bottom window, and injection plate in the 31M10 and (b) a mock-up of the 31M10 test section constructed in the lab.

B. Supersonic Retropropulsion Model Considerations

In order to optimize the camera placement around the full-scale mock-up test section and obtain preliminary time-resolved density field reconstructions from the tomographic BOS measurement system in the laboratory, an SRP model was needed that would aid in camera alignment and provide a gas jet similar in nature to the counter-flowing jet observed during tunnel testing. Since only the flow upstream of the actual SRP model's forebody is of interest in the final test, and to avoid damaging the electronic instrumentation already mounted in the actual SRP model, a 3D-printed forebody model was fabricated using Formlabs'™ Durable resin with the same dimensions as the actual SRP model. Figure 5 shows this forebody model. In this image a 60° full-cone spray nozzle (McMaster-Carr®, 32885K143) was embedded in the forebody model at the same location as the central nozzle in the actual SRP model. This nozzle was connected to a pipe that extended out of the back of the forebody model and could be connected to a pressurized helium gas bottle or compressed air line to produce a jet flow similar to that which would be observed in the tunnel test.

C. High-Intensity Pulsed Illumination

During preliminary high-speed tomographic BOS testing in 2019, it was difficult to obtain uniform illumination over the entire field-of-view with sufficient intensity at framing rates above 20 kHz when using a patterned retroreflective background. This was a consequence of the central axis of the LED light source not being aligned with the optical axis of the camera as well as the limited output intensity of the pulsed LED. To improve the uniformity and return intensity of the illumination, a new illumination module was developed and is shown in Fig. 6. This module consisted of a 3D-printed housing that was secured in a kinematic mirror mount (Thorlabs™, KM200) to provide for adjustment of the incidence angle of the illumination source's axis on the patterned retroreflective background. Illumination for this module is provided by one of seven 2.5-m-long optical fibers from a fiber bundle that connects to a Cavitar™ Cavilux HF laser illumination source operating at 640 nm. The fiber connects to the rear of the module via an SMA terminated fiber adapter (Thorlabs™, SM05SMA) threaded into a flange (Thorlabs™, SM05F1) that bolts onto the back end of the 3D-printed housing as shown in Fig. 6a. The light exiting the fiber is then loosely collimated and diffused by a condenser/diffuser lens (Thorlabs™, ACL5040U-DG15-A) secured inside a flange (Thorlabs™, SM2F1)

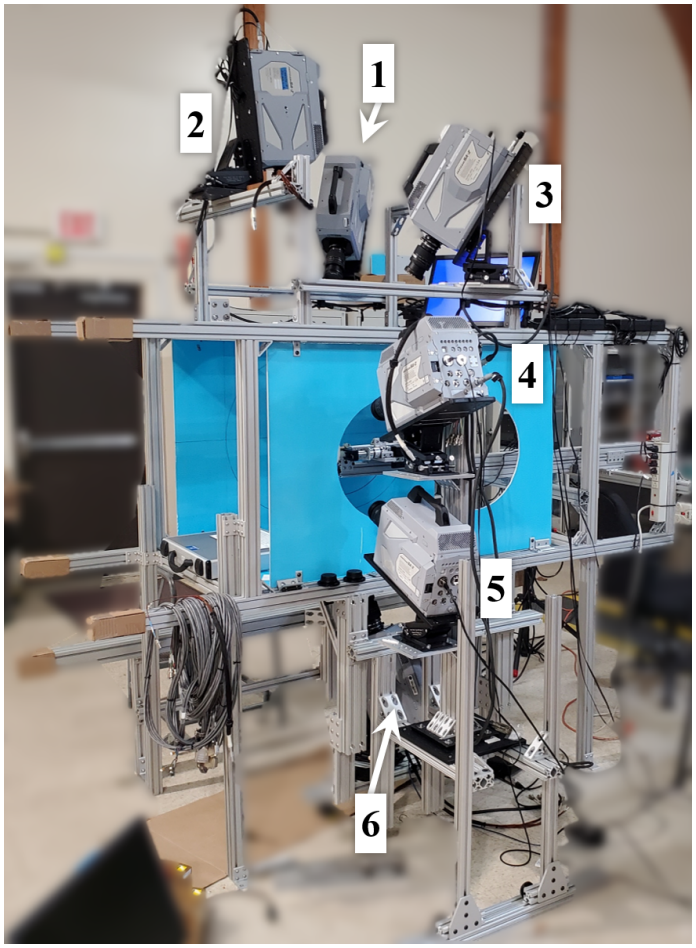

Fig. 4 31M10 laboratory mock-up with six high-speed cameras mounted around the test section.

bolted to the 3D-printed housing. This light was then reflected onto the camera's optic axis by a 75-mm-square 50:50 plate beamsplitter (Edmund Optics®, #48-904) mounted in the 3D-printed housing oriented at a 45° relative to the camera's optic axis, as shown in Fig. 6b. The light is then projected onto a patterned retroreflective background (3M™ Scotchlite™, 7610WS) where it is reflected back to the camera. This is shown in Fig. 6c, where the patterned retroreflective background was placed approximately 1.3 m from the imaging system, similar to the spacing used in the lab mock-up of the 31M10.

Figure 7 shows a montage of images acquired with the Photron™ SA-Z camera viewing the patterned retroreflective background through the fiber illuminator module as shown in Fig. 6c. Each image in the montage was acquired with a different leg of the 7-fiber bundle attached to the Cavitar™ Cavilux HF pulsed laser light source with 260 ns pulse widths. A 260 ns pulse width was selected as it is the maximum pulse width that can be achieved with the laser source when operating at 75 kHz. All of the legs of the fiber bundle converge at the laser source in a 6-around-1 bundle configuration, where six outer fiber ends (fibers A-F) surround a center fiber end. Each fiber has a core diameter of 0.5 mm and is 2.5 m in length. While the intensity and uniformity from each fiber differs, the mean signal intensity in each image ranged from 1/4 to 1/2 of the dynamic range of the camera, which is more than sufficient to acquire BOS image data. Adjustments to the condenser/diffuser lens position in the fiber illuminator module may also be made to further improve uniformity of the illumination. If even higher intensities are required, the framing rate of the camera (and therefore pulse rate of the laser illumination source) can be reduced and the pulse width extended. Note that the full sensor size of 1024×1024 pixels was used to acquire the images in Fig. 7, whereas a reduced sensor size of 512×456 pixels will be used to achieve a framing rate of 75 kHz, effectively cropping out the regions of reduced intensity observed in these images.

Figure 8a shows a raw BOS image of a heat gun placed midway between the patterned retroreflective background

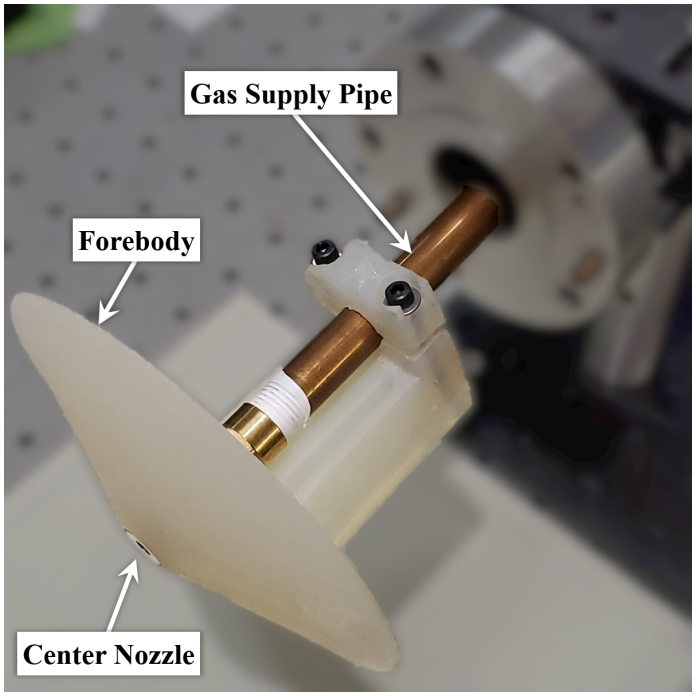

Fig. 5 3D-printed SRP 70° sphere-cone model forebody with center nozzle and gas supply pipe.

and imaging system using the center fiber of the 7-fiber bundle for illumination. Figure 8b shows the resulting 2D displacement map computed using LaVision's™ DaVis 10 2D BOS software module. An 11-pixel subset window size with a 3-pixel subset window overlap was used to process the data. A mask has also been applied over the silhouette of the heat gun nozzle. This analysis demonstrates that relatively high-quality 2D BOS images can be acquired with the imaging system setup, which includes the high-speed camera and fiber illuminator module shown in Fig. 6.

In the event that the six single-view, high-speed imaging systems do not provide for a sufficiently high-quality volumetric density field reconstruction, a frame splitter may be used to double the number of views that can be obtained with each system. An example of a frame splitter mounted in front of a high-speed Photron™ SA-Z camera is shown in Fig. 9. Here, a 50-mm 90° right-angle specialty mirror (Edmund Optics®, #47-006) is used to redirect the view of the left- and right-hand sides of the imaging sensor onto two LED-based illuminator modules. For tests in the 31M10 mock-up, these LED-based illuminator modules will be replaced with the fiber-based illuminator modules shown in Fig. 6. A second laser head and 7-fiber bundle would then be used to provide pulsed laser illumination for at least six frame splitters (with a total of twelve fiber illuminator modules).

D. Retroreflective Background Application on Tunnel Walls

The limited optical access of the 31M10 will require some of the patterned retroreflective material to be mounted on the interior walls and on the injection plate of the facility. For this tomographic BOS test, 3M™ Scotchlite™ 7610 retroreflective sheeting will be used as the primary background. However, the delicate nature of the material and the difficulty associated with its application to surfaces requires the use of a separate 3M™ 1080 vinyl backing material that allows for easier application and removal. The use of these two materials was initially proposed and used by JT Heineck at NASA's Ames Research Center and used successfully for tomographic BOS measurements in the 11-by-11-Foot Transonic Wind Tunnel at Ames as is detailed in Ref. [28].

While the use of the layered 3M™ 1080 vinyl wrap material and Scotchlite™ 7610 retroreflective material makes it easier to apply and remove from the wind tunnel walls, it was unclear if it could survive the high temperatures encountered in the 31M10 test section during pre-heating (a procedure where high temperature air is cycled through the tunnel stagnation chamber and test section to bring components up to operating temperatures) and testing. To determine if these layered materials could survive in the tunnel environment, a laboratory test was performed where the layered materials were mounted onto a water-cooled metal slab (approximating the water-cooled walls of the 31M10)

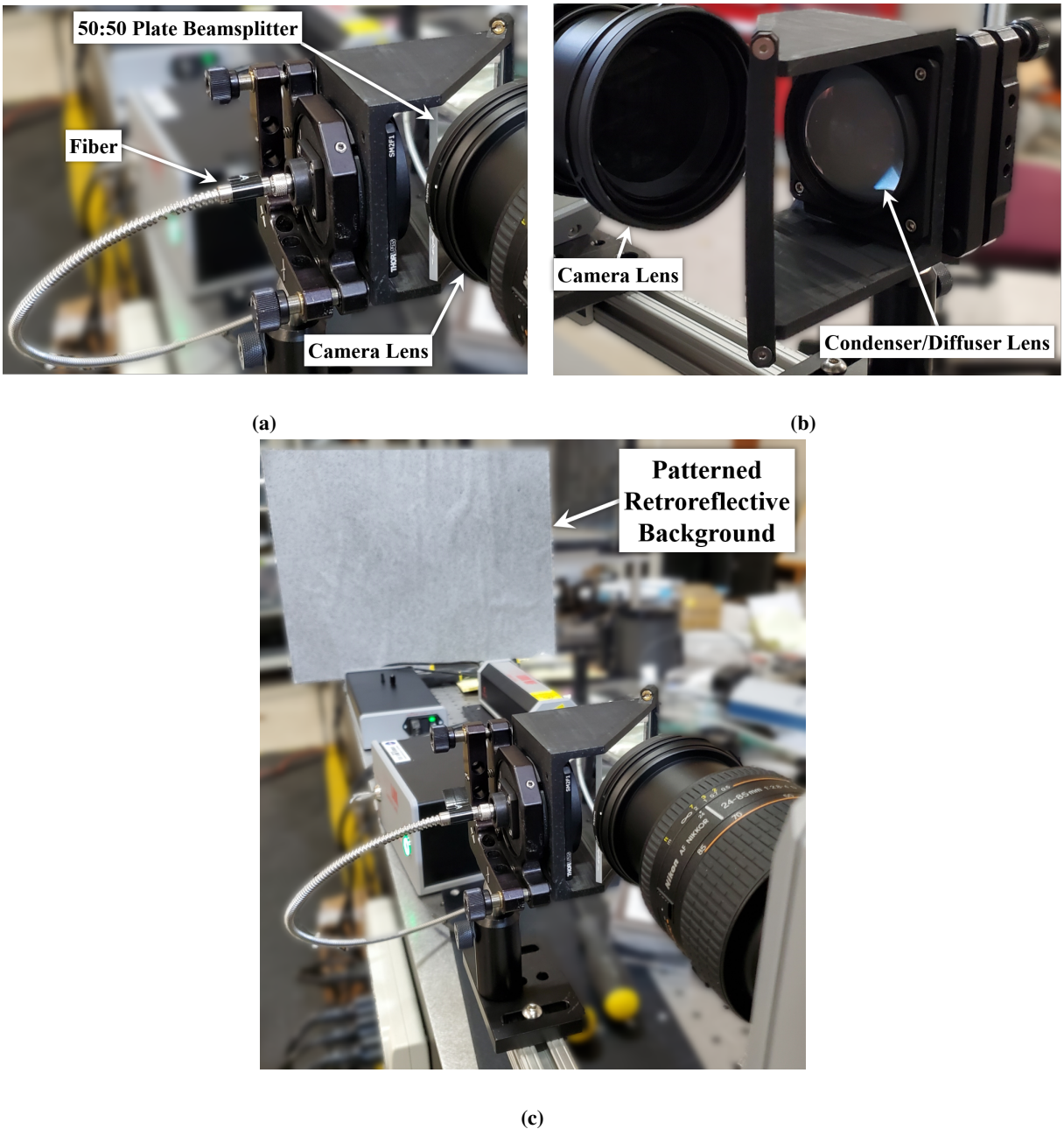

Fig. 6 (a) View of the rear of the fiber illuminator module, (b) perspective view of camera facing laser fiber illuminator module, and (c) zoomed-out view of (a) showing imaging system viewing a patterned retroreflective background through fiber illuminator module.

and exposed to high temperature air from two heat guns over a 45 minute period (corresponding to the initial pre-heat procedure performed at the beginning of each test day). Thermocouples were used to monitor the air temperature immediately above the layered materials and at different locations on the metal slab. A camera mounted above the metal slab was used to image the top surface of the retroreflective material to observe the development of any damage resulting from heating. This experimental setup is shown in Fig. 10a.

Interestingly, measurements of the static temperature in the 31M10 test section during an initial long pre-heat procedure and a short inter-run pre-heat procedure (performed between runs of the wind tunnel during a standard test day) had never been performed, and the peak temperature and rate of temperature increase were unknown. As a

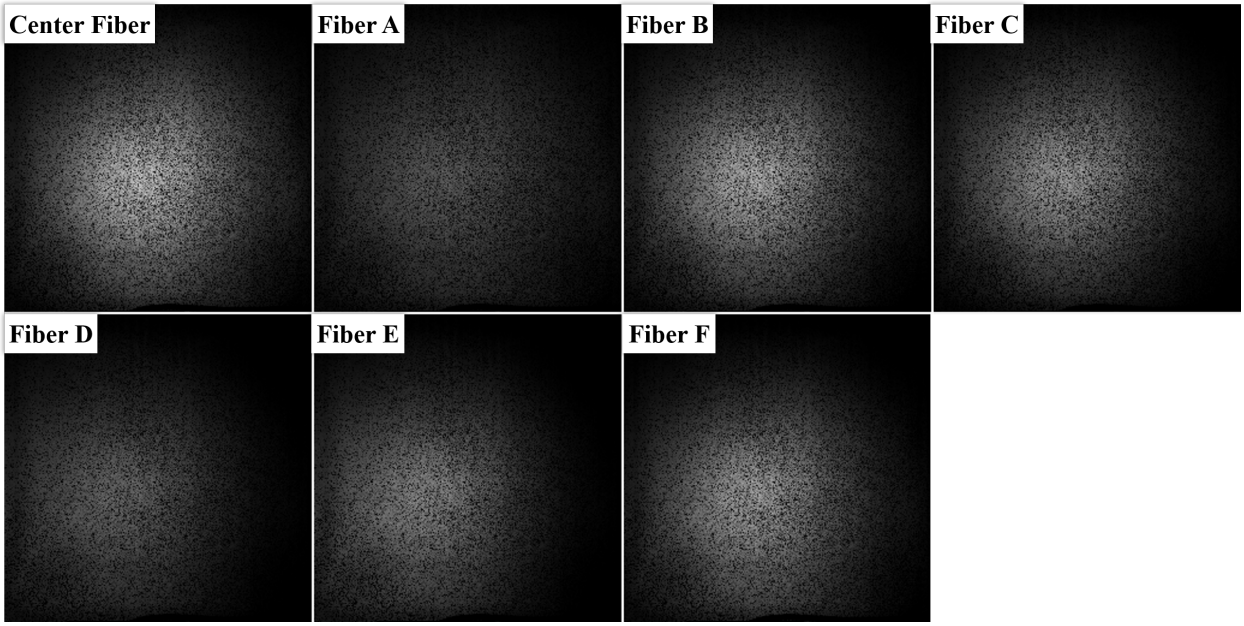

Fig. 7 Montage of raw images of patterned retroreflective background obtained with each fiber in 7-fiber bundle.

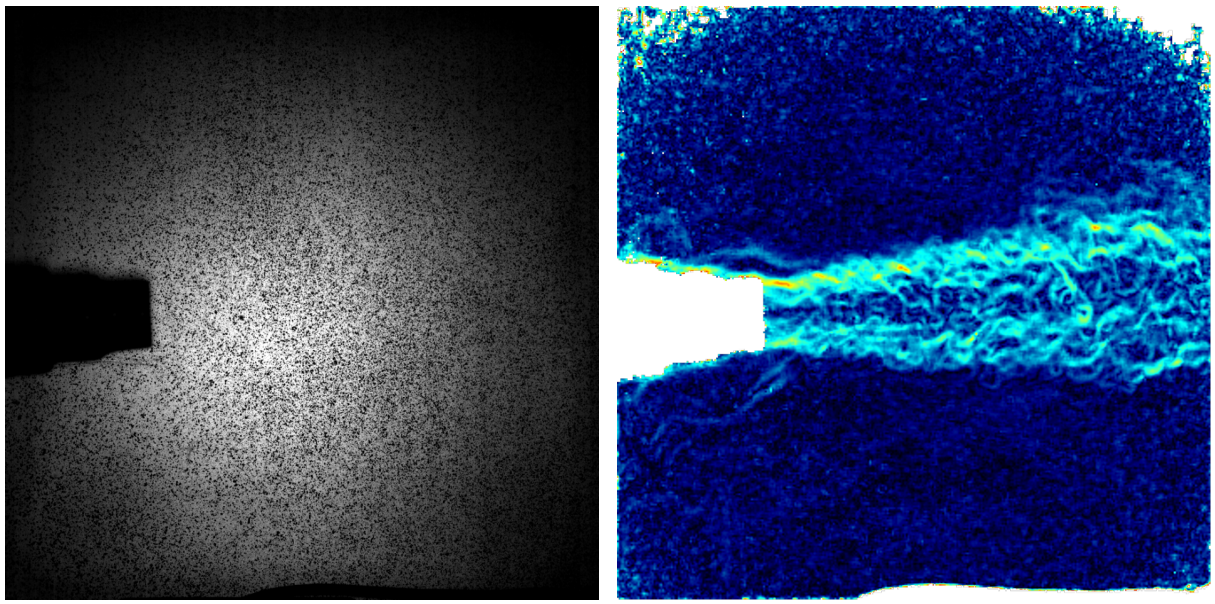

(a) **(b)**

Fig. 8 (a) Raw and (b) processed BOS image obtained with Photron™ SA-Z camera and illumination module.

result, measurements of the test section static temperature during these procedures were performed using a fine tip thermocouple (Omega™, TJFT72-K-SS-116G-6-SMPW-M) that was inserted into the test section through a port on the top wall of the tunnel, just upstream of the top window. This thermocouple was inserted approximately 50.8 mm into the flow relative to the top interior wall surface. These temperature measurements are presented in Fig. 10b and are denoted by the blue data points. These measurements showed that during both the initial long pre-heat and regular short pre-heat procedures, the static air temperature in the tunnel's test section never exceeds 600 °F. During the initial

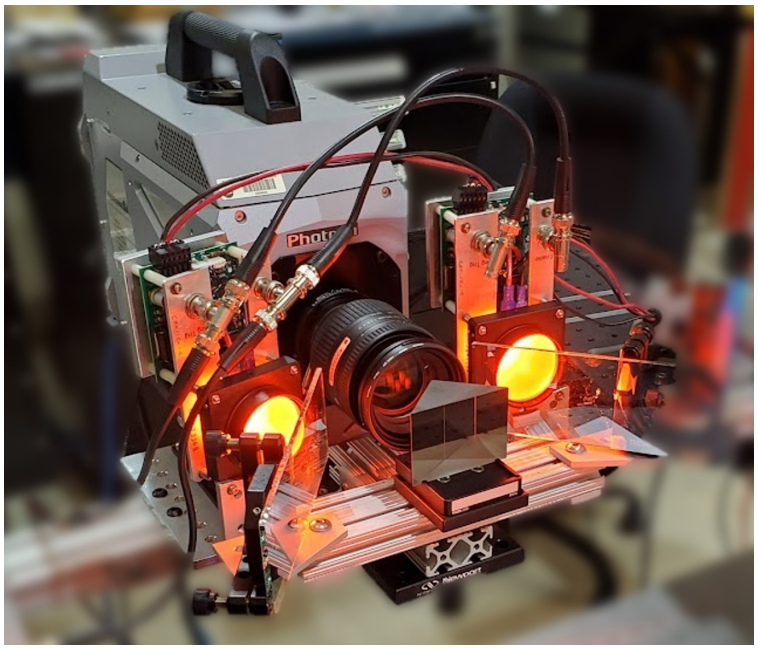

Fig. 9 High-speed camera with frame splitter using two LED-based illuminator modules. These modules will be replaced with the fiber-based illuminator modules shown in Fig. 6.

pre-heat procedure, the heating rate is also relatively slow, with the peak temperature being achieved after approximately 40 minutes. The solid yellow line in this plot denotes the static air temperature above the layered materials measurement in the laboratory setup shown in Fig. 10a. The dashed yellow line in this plot denotes the temperature recorded by a thermocouple placed at the metal slab surface (shown in the middle of the layered materials in Fig. 10a). This plot shows that the static air temperature in laboratory tests exceeded those encountered in the wind tunnel test section during pre-heat procedures. Further, the pressure in the wind tunnel test section during these pre-heat procedures was approximately 6 psia, whereas the pressure in the laboratory test was atmospheric pressure (14.7 psia). Since no damage was observed in the layered materials and the vinyl wrap material retained its tackiness on the adhering side when removed from the cooled metal slab after testing, confidence was gained that the layered materials would survive in the 31M10 test section when used for high-speed tomographic BOS testing.

E. Tomographic BOS Calibration System

Physical access to the test section of the 31M10 is typically provided by opening the side window. Since the placement of high-speed cameras next to the side window will prevent entry to the test section, an alternative method of maneuvering a calibration target about the measurement volume inside the test section is required. Figure 11 shows the proposed remotely-controlled calibration system mounted in the mock-up of the test section that will eventually be used for the high-speed tomographic BOS tests in the actual facility. This system consists of an 80/20™ structure that clamps to the 50.8-mm-diameter SRP sting using a pair of U-bolts. A Zaber™ X-NMS17-C stepper motor coupled to a SureGear® PGCN17-105M gearbox allows for remote rotation adjustment of a LaVision™ QR5-306-11.6 calibration target attached to the shaft of the gearbox. An image of the calibration system and calibration target as viewed from the side window (looking slightly upstream) of the tunnel mock-up is shown in Fig. 11a.

When in use in the actual wind tunnel, the system will be clamped to the model sting and the model will be manually inserted into the tunnel test section using the model injection system such that the rotation axis of the calibration target corresponds to the SRP model's jet axis. The calibration target is then rotated about this axis so that several images of the calibration target at different orientations are acquired for each camera view. For testing in the mock-up, a 50.8-mm-diameter stud was used to mimic the SRP model's sting, allowing the calibration system to be attached to the mock-up model using the aforementioned U-bolts. This is most clearly seen in Fig. 11b, which shows an image of

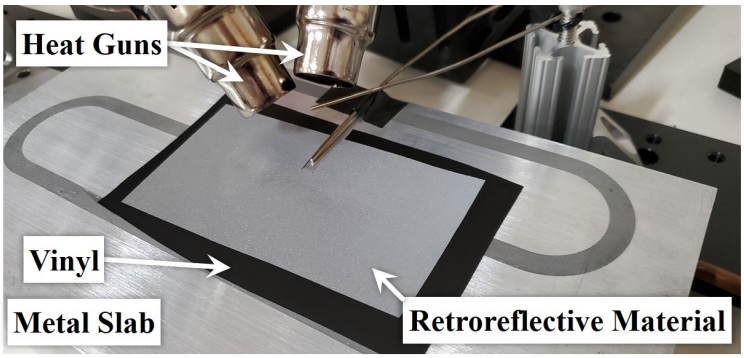

(a)

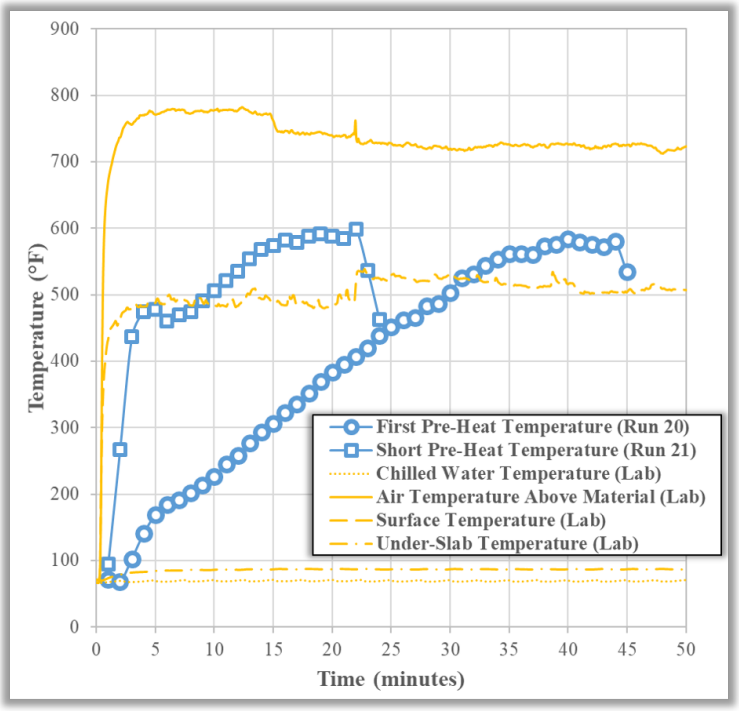

(b)

Fig. 10 (a) Laboratory testing of layered retroreflective and vinyl materials and (b) comparison of measurements obtained in the lab (yellow curves) versus those obtained in the 31M10 test section during pre-heats (blue curves with data points).

the mock-up SRP model with the calibration system attached as viewed from the top window of the facility mock-up (looking slightly downstream). For calibration in the mock-up facility, the strut assembly will be adjusted such that the rotation axis of the calibration system is positioned along the centerline.

III. Future Work

Several issues have yet to be addressed in the 31M10 mock-up prior to executing the final test at the actual facility. With the cameras mounted around the mock-up and aligned, a check will first be performed to ensure that window reflections do not interfere with the image data obtained with each camera system. This check will consist of placing a

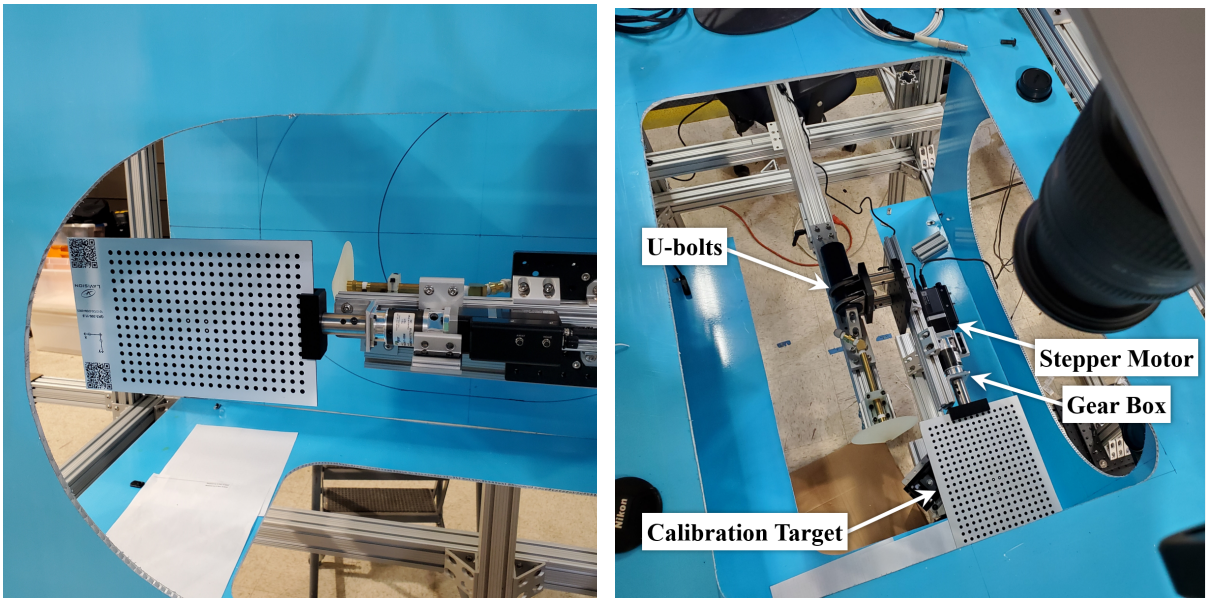

(a) (b)

Fig. 11 Comparison views from the (a) side and (b) top window of the calibration system in the 31M10 test section mock-up.

piece of transparent acrylic over each window and looking for any reflections. If a reflection is observed in any of the camera views, the alignment of the camera will be adjusted to eliminate it.

The next most significant challenge will be to pattern numerous pieces of the retroreflective material and mount them in the mock-up. In order to properly size and space the dots of the pattern, the magnification of the imaging systems when viewing the backgrounds will need to be established. This will be accomplished by placing the calibration target on the surfaces where the material will ultimately be mounted and capture images of the target to determine magnification. The current method of applying the dot pattern at Langley consists of drilling out the nozzle of a high-temperature BBQ spray paint can and then spraying the material, taking care to ensure uniformity of the pattern size, spacing, and density. This was discussed in Refs. [26, 28]. An alternative method of applying a dot pattern to the material has been developed by JT Heineck at NASA Ames Research Center, where screen printing is used to ensure highly controlled dot sizing and spacing on the retroreflective material, also discussed in Ref. [28]. Unfortunately, both of these pattern application methods do not allow for changes to be made once the pattern has been applied. While the use of laser speckle as the pattern has shown to be effective in laboratory settings [40, 41], the vibrations in a test facility are often significant enough to cause shot-to-shot variations in the projected speckle pattern, limiting the effectiveness of the approach. A new projection BOS method [42] that overcomes these challenges may be considered for use in this test campaign. This method allows for on-the-fly changes to the pattern and offers a reference-free BOS imaging capability.

Once a pattern has been applied to the retroreflective material and mounted inside of the mock-up test section, a series of tomographic BOS experiments will be performed in the mock-up test section to ensure that the volumetric reconstruction sufficiently covers the volume of interest, and that the smallest scales achieved with the volumetric reconstructions are equal to, or smaller than, those that will need to be resolved in the final test campaign. Currently, the plan is to use LaVision's™ DaVis 2D BOS software module to compute the 2D displacement maps. However, if it is determined that finer BOS resolution is needed, an optical flow algorithm similar to that described in Refs. [6, 7] may be incorporated to achieve 2D displacement maps with single-pixel resolution.

Finally, while two Cavitar™ Cavilux HF lasers and two sets of 7-fiber bundles are available for illumination of the patterned retroreflective backgrounds, two 4-fiber bundles have also been purchased that offer larger core diameters and therefore higher intensity compared to the 7-fiber bundles. These will also be evaluated in the mock-up test section tests.

IV. Conclusions

A discussion on the work being performed in preparation for an anticipated high-speed tomographic background-oriented schlieren (BOS) test in NASA Langley Research Center's 31-Inch Mach 10 wind tunnel has been provided in this paper. This work included the construction of a full-scale mock-up of the wind tunnel facility complete with properly sized and positioned window access. This mock-up allowed for the camera systems to be aligned and focused for optimal tomographic BOS reconstruction data, reducing the setup time and any troubleshooting in the facility required prior to the test. A full-scale replica of the supersonic retropropulsion wind tunnel model was 3D-printed and fitted with a nozzle that could be connected to a pressurized gas supply, allowing for visualization of high-pressure jets from the model with the tomographic BOS system. To provide time-resolved visualization of the jet flow, a pulsed laser illumination system was coupled to a 7-fiber bundle, with six of the fiber ends coupled to an illumination module that conditioned the light exiting the fiber and coupled it onto the optical axis of each camera using a 50:50 plate beamsplitter. This arrangement enabled relatively high-quality 2D BOS images to be obtained with laser pulse widths of 260 ns. Work was also performed to ensure that the patterned retroreflective material that will be used for the BOS background could survive the high temperatures present in the facility test section. A remotely-controlled calibration system was also developed that allows for remote adjustment of a calibration target for volumetric calibration of the tomographic BOS system. While additional work must be performed prior to the test campaign, the preparations discussed in this paper have demonstrated that the outlined approach will be sufficient for obtaining high-quality tomographic BOS data.

Acknowledgments

This work was funded by NASA's Transformational Tools and Technologies (T^3) and Aerosciences Evaluation and Test Capabilities (AETC) projects.

References

[1] Raffel, M., "Background-oriented schlieren (BOS) techniques," *Experiments in Fluids*, Vol. 56, No. 3, 2015. https://doi.org/10.1007/s00348-015-1927-5.

[2] Dalziel, S. B., Hughes, G. O., and Sutherland, B. R., "Whole-field density measurements by 'synthetic schlieren'," *Experiments in Fluids*, Vol. 28, No. 4, 2000, pp. 322–335. https://doi.org/10.1007/s003480050391.

[3] Raffel, M., Richard, H., and Meier, G. E. A., "On the applicability of background oriented optical tomography for large scale aerodynamic investigations," *Experiments in Fluids*, Vol. 28, No. 5, 2000, pp. 477–481. https://doi.org/10.1007/s003480050408.

[4] Raffel, M., Tung, C., Richard, H., Yu, Y., and Meier, G., "Background oriented stereoscopic schlieren (BOSS) for full scale helicopter vortex characterization," *9th International Symposium on Flow Visualization*, 2000, pp. 23–24.

[5] Meier, G., "Computerized background-oriented schlieren," *Experiments in Fluids*, Vol. 33, No. 1, 2002, pp. 181–187. https://doi.org/10.1007/s00348-002-0450-7.

[6] Schmidt, B. E., and Woike, M. R., "Wavelet-Based Optical Flow Analysis for Background-Oriented Schlieren Image Processing," *AIAA Journal*, Vol. 59, No. 8, 2021, pp. 3209–3216. https://doi.org/10.2514/1.j060218.

[7] Smith, N. T., Heineck, J. T., and Schairer, E. T., "Optical Flow for Flight and Wind Tunnel Background Oriented Schlieren Imaging," *55th AIAA Aerospace Sciences Meeting*, American Institute of Aeronautics and Astronautics, 2017. https://doi.org/10.2514/6.2017-0472, AIAA Paper 2017-0472.

[8] Atcheson, B., Ihrke, I., Heidrich, W., Tevs, A., Bradley, D., Magnor, M., and Seidel, H.-P., "Time-resolved 3d capture of non-stationary gas flows," *ACM Transactions on Graphics*, Vol. 27, No. 5, 2008, pp. 1–9. https://doi.org/10.1145/1409060.1409085.

[9] Venkatakrishnan, L., and Suriyanarayanan, P., "Density field of supersonic separated flow past an afterbody nozzle using tomographic reconstruction of BOS data," *Experiments in Fluids*, Vol. 47, No. 3, 2009, pp. 463–473. https://doi.org/10.1007/s00348-009-0676-8.

[10] Zeb, M. F., Ota, M., and Maeno, K., "Quantitative measurement of heat flow in natural heat convection using color-stripe background oriented schlieren (CSBOS) method," *Journal of the Japanese Society for Experimental Mechanics*, Vol. 11, 2011, pp. s141–s146. Special Issue.

[11] Ota, M., Hamada, K., Kato, H., and Maeno, K., "Computed-tomographic density measurement of supersonic flow field by colored-grid background oriented schlieren (CGBOS) technique," *Measurement Science and Technology*, Vol. 22, No. 10, 2011, p. 104011. https://doi.org/10.1088/0957-0233/22/10/104011.

[12] Todoroff, V., Plyer, A., Besnerais, G. L., Champagnat, F., Donjat, D., Micheli, F., and Millan, P., "3D reconstruction of the density field of a jet using synthetic BOS images," *CD-Proc. 15th Int. Symp. on Flow Visualization*, 2012.

[13] Sourgen, F., Leopold, F., and Klatt, D., "Reconstruction of the density field using the Colored Background Oriented Schlieren Technique (CBOS)," *Optics and Lasers in Engineering*, Vol. 50, No. 1, 2012, pp. 29–38. https://doi.org/10.1016/j.optlaseng.2011.07.012.

[14] Leopold, F., Ota, M., Klatt, D., and Maeno, K., "Reconstruction of the Unsteady Supersonic Flow around a Spike Using the Colored Background Oriented Schlieren Technique," *Journal of Flow Control, Measurement, & Visualization*, Vol. 01, No. 02, 2013, pp. 69–76. https://doi.org/10.4236/jfcmv.2013.12009.

[15] Adamczuk, R. R., Hartmann, U., and Seume, J., "Experimental Demonstration of Analyzing an Engine's Exhaust Jet with the Background-Oriented Schlieren Method," *AIAA Ground Testing Conference*, American Institute of Aeronautics and Astronautics, 2013. https://doi.org/10.2514/6.2013-2488, AIAA Paper 2013-2488.

[16] Todoroff, V., Le Besnerais, G., Donjat, D., Micheli, F., Plyer, A., and Champagnat, F., "Reconstruction of instantaneous 3D flow density fields by a new direct regularized 3DBOS method," *17th International Symposium on Applications of Laser Techniques to Fluid Mechanics*, 2014, pp. 1–12.

[17] Donjat, D., Nicolas, F., Plyer, A., Micheli, F., Cornic, P., Le Besnerais, G., Champagnat, F., Le Sant, Y., and Deluc, J.-M., "Study of a co-flowing hot jet: an application of direct 3DBOS technique in research wind tunnel," *10th Pacific Symposium on Flow Visualization and Image Processing, Naples, Italy Google Scholar*, 2015.

[18] Hartmann, U., Adamczuk, R., and Seume, J., "Tomographic Background Oriented Schlieren Applications for Turbomachinery (Invited)," *53rd AIAA Aerospace Sciences Meeting*, American Institute of Aeronautics and Astronautics, 2015. https://doi.org/10.2514/6.2015-1690, AIAA Paper 2015-1690.

[19] Hartmann, U., and Seume, J. R., "Combining ART and FBP for improved fidelity of tomographic BOS," *Measurement Science and Technology*, Vol. 27, No. 9, 2016, p. 097001.

[20] Nicolas, F., Donjat, D., Plyer, A., Champagnat, F., Besnerais, G. L., Micheli, F., Cornic, P., Sant, Y. L., and Deluc, J. M., "Experimental study of a co-flowing jet in ONERA's F2 research wind tunnel by 3D background oriented schlieren," *Measurement Science and Technology*, Vol. 28, No. 8, 2017, p. 085302. https://doi.org/10.1088/1361-6501/aa7827.

[21] Nicolas, F., Donjat, D., Léon, O., Besnerais, G. L., Champagnat, F., and Micheli, F., "3D reconstruction of a compressible flow by synchronized multi-camera BOS," *Experiments in Fluids*, Vol. 58, No. 5, 2017. https://doi.org/10.1007/s00348-017-2325-y.

[22] Grauer, S. J., Unterberger, A., Rittler, A., Daun, K. J., Kempf, A. M., and Mohri, K., "Instantaneous 3D flame imaging by background-oriented schlieren tomography," *Combustion and Flame*, Vol. 196, 2018, pp. 284–299. https://doi.org/10.1016/j.combustflame.2018.06.022.

[23] Zhang, L., Song, Y., Qu, X., Li, Z., and He, A., "Quantitative reconstruction of 3D flow density fields by a direct computerized tomography method of BOS," *Optical Metrology and Inspection for Industrial Applications V*, edited by S. Han, T. Yoshizawa, and S. Zhang, SPIE, 2018. https://doi.org/10.1117/12.2500760.

[24] Amjad, S., Soria, J., and Atkinson, C., "Time-averaged three-dimensional density and temperature field measurement of a turbulent heated jet using background-oriented schlieren," *21st Australasian Fluid Mechanics Conference, Adelaide, December*, 2018.

[25] Nicolas, F., Donjat, D., Micheli, F., Le Besnerais, G., Plyer, A., Cornic, P., Champagnat, F., and Michou, Y., "Experimental study of a counter-flow jet in ONERA's S1MA wind tunnel by 3D background oriented schlieren," *ISFV 18*, 2018.

[26] Bathel, B. F., Weisberger, J., and Jones, S. B., "Development of Tomographic Background-Oriented Schlieren Capability at NASA Langley Research Center," American Institute of Aeronautics and Astronautics, 2019. https://doi.org/10.2514/6.2019-3288, AIAA Paper 2019-3288.

[27] Liu, H., Shui, C., and Cai, W., "Time-resolved three-dimensional imaging of flame refractive index via endoscopic background-oriented schlieren tomography using one single camera," *Aerospace Science and Technology*, Vol. 97, 2020, p. 105621. https://doi.org/10.1016/j.ast.2019.105621.

[28] Weisberger, J. M., Bathel, B. F., Jones, S. B., Woike, M. R., Ponder, J. D., Heineck, J. T., and Schairer, E. T., "Preparations for Tomographic Background-Oriented Schlieren Measurements in the 11-by 11-Foot Transonic Wind Tunnel," American Institute of Aeronautics and Astronautics, 2020. https://doi.org/10.2514/6.2020-3102, AIAA Paper 2020-3102.

[29] Amjad, S., Karami, S., Soria, J., and Atkinson, C., "Assessment of three-dimensional density measurements from tomographic background-oriented schlieren (BOS)," *Measurement Science and Technology*, Vol. 31, No. 11, 2020, p. 114002. https://doi.org/10.1088/1361-6501/ab955a.

[30] Grauer, S. J., and Steinberg, A. M., "Fast and robust volumetric refractive index measurement by unified background-oriented schlieren tomography," *Experiments in Fluids*, Vol. 61, No. 3, 2020. https://doi.org/10.1007/s00348-020-2912-1.

[31] Davis, J. K., Clifford, C. J., Kelly, D. L., and Thurow, B. S., "Tomographic background oriented schlieren using plenoptic cameras," *Measurement Science and Technology*, Vol. 33, No. 2, 2021, p. 025203. https://doi.org/10.1088/1361-6501/ac3b09.

[32] Unterberger, A., and Mohri, K., "Evolutionary background-oriented schlieren tomography with self-adaptive parameter heuristics," *Optics Express*, Vol. 30, No. 6, 2022, p. 8592. https://doi.org/10.1364/oe.450036.

[33] Gomez, M., Grauer, S. J., Ludwigsen, J., Steinberg, A. M., Son, S. F., Roy, S., and Meyer, T. R., "Megahertz-rate background-oriented schlieren tomography in post-detonation blasts," *Applied Optics*, Vol. 61, No. 10, 2022, p. 2444. https://doi.org/10.1364/ao.449654.

[34] Cai, S., Wang, Z., Fuest, F., Jeon, Y. J., Gray, C., and Karniadakis, G. E., "Flow over an espresso cup: inferring 3-D velocity and pressure fields from tomographic background oriented Schlieren via physics-informed neural networks," *Journal of Fluid Mechanics*, Vol. 915, 2021. https://doi.org/10.1017/jfm.2021.135.

[35] Karniadakis, G. E., Kevrekidis, I. G., Lu, L., Perdikaris, P., Wang, S., and Yang, L., "Physics-informed machine learning," *Nature Reviews Physics*, Vol. 3, No. 6, 2021, pp. 422–440. https://doi.org/10.1038/s42254-021-00314-5.

[36] Bathel, B. F., Litzner, C. R., Jones, S. B., Berry, S. A., Smith, N. T., and Garbeff, T. J., "High-Speed Schlieren Analysis of Retropropulsion Jet in Mach 10 Flow," Vol. 57, No. 1, 2020, pp. 33–48. https://doi.org/10.2514/1.a34522.

[37] Berry, S. A., and Rhode, M., "Supersonic Retropropulsion Test 1853 in NASA LaRC Unitary Plan Wind Tunnel Test Section 2," Technical Report 2014-218256, Apr. 2014.

[38] Micol, J., "Langley Aerothermodynamic Facilities Complex - Enhancements and Testing Capabilities," American Institute of Aeronautics and Astronautics, 1998. https://doi.org/10.2514/6.1998-147, AIAA Paper 1998-147.

[39] Berger, K. T., Hollingsworth, K. E., Wright, S. A., and Rufer, S. J., "NASA Langley Aerothermodynamics Laboratory: Hypersonic Testing Capabilities," *53rd AIAA Aerospace Sciences Meeting*, American Institute of Aeronautics and Astronautics, 2015. https://doi.org/10.2514/6.2015-1337, AIAA Paper 2015-1337.

[40] Meier, A. H., and Roesgen, T., "Improved background oriented schlieren imaging using laser speckle illumination," *Experiments in Fluids*, Vol. 54, No. 6, 2013. https://doi.org/10.1007/s00348-013-1549-8.

[41] Kushner, L. K., Heineck, J. T., Storms, B. L., and Childs, R., "Visualization of a Sweeping Jet by Laser Speckle Retro-reflective Background Oriented Schlieren," *53rd AIAA Aerospace Sciences Meeting*, American Institute of Aeronautics and Astronautics, 2015. https://doi.org/10.2514/6.2015-1697, AIAA Paper 2015-1697.

[42] Weisberger, J. M., and Bathel, B. F., "Projection Background-Oriented Schlieren," *2022 AIAA Aviation Forum*, American Institute of Aeronautics and Astronautics, 2022.